Bioorganic & Medicinal Chemistry 19 (2011) 1683–1691

Contents lists available at ScienceDirect

Bioorganic & Medicinal Chemistry

journal homepage: www.elsevier.com/locate/bmc

Biological activity and ligand binding mode to the progesterone receptor of A-homo analogues of progesterone

Lautaro D. Alvarez [a,b], María V. Dansey [a], Marcelo A. Martí [c,d], Paola Y. Bertucci [b], Pablo H. Di Chenna [a], Adalí Pecci [b,c], Gerardo Burton [a,*]

[a] Departamento de Química Orgánica and UMYMFOR (CONICET-UBA), Facultad de Ciencias Exactas y Naturales, Universidad de Buenos Aires, Pabellón 2, Ciudad Universitaria, C1428EGA Buenos Aires, Argentina
[b] IFIBYNE (CONICET-UBA), Facultad de Ciencias Exactas y Naturales, Universidad de Buenos Aires, Pabellón 2, Ciudad Universitaria, C1428EGA Buenos Aires, Argentina
[c] Departamento de Química Biológica (UBA), Facultad de Ciencias Exactas y Naturales, Universidad de Buenos Aires, Pabellón 2, Ciudad Universitaria, C1428EGA Buenos Aires, Argentina
[d] INQUIMAE (CONICET-UBA), Facultad de Ciencias Exactas y Naturales, Universidad de Buenos Aires, Pabellón 2, Ciudad Universitaria, C1428EGA Buenos Aires, Argentina

ARTICLE INFO

Article history:
Received 18 November 2010
Revised 11 January 2011
Accepted 16 January 2011
Available online 22 January 2011

Keywords:
Progesterone receptor
A-Homo pregnane
Molecular dynamics
Progestagen

ABSTRACT

The biological activity of two seven-membered A-ring (A-homo) analogues of progesterone was evaluated by transactivation assays in Cos-1 cells and by determination of Bcl-x_L expression levels in T47D cells. The results show that both compounds act as selective progesterone receptor (PR) agonists but lack mineralocorticoid receptor (MR) activity. Molecular modelling using semiempirical AM1 and ab initio HF/6-31G** calculations, showed that the A-ring of the A-homo steroids may adopt five different conformations, although only three correspond to low energy conformers. The low energy conformers of each analogue were introduced into the ligand binding pocket of the PR ligand binding domain (LBD) obtained from the PR LBD–progesterone crystal structure. The steroid binding mode was then analyzed using 10 ns of molecular dynamics (MD) simulation. The PR LBD–progesterone complex was also simulated as a control system. The MD results showed that both A-homo steroids have one conformer that may be properly recognized by the PR, in agreement with the observed progestagen activity. Moreover, the simulation revealed the importance of a water molecule in the formation of a hydrogen bonding network among specific receptor residues and the steroid A-ring carbonyl.

1. Introduction

Progesterone (**1**) is a steroid hormone that exerts a wide variety of biological effects in mammalian organisms. It is involved in the female menstrual cycle, having many roles relating to pregnancy and embryogenesis. In particular, progesterone converts the endometrium to its secretory stage to prepare the uterus for implantation.[1] It also contributes to mammary gland development and lactation inhibition during pregnancy.[2] On the other hand, progesterone can be synthesized within the central nervous system where it affects synaptic functioning and myelination.[3,4] Among other effects, progesterone also regulates the expression of apoptotic and proliferative genes, acts as an antiinflammatory agent and regulates the immune response.[5,6] Physiological effects of progesterone are mediated by multiple mechanisms of action; mainly through the activation of the progesterone receptor (PR),[7] a member of the oxosteroid receptor family (oSR), which also includes receptors for the mineralocorticoids (MR), glucocorticoids (GR) and androgens (AR).[8] The oSRs are soluble intracellular proteins that act mainly as ligand regulated transcription factors, regulating specific gene expression in most mammalian cells.[9]

Structurally, oSRs are modular proteins organized into three major domains: an N-terminal activation function-1 (AF-1), a central DNA binding domain (DBD) and a C-terminal ligand binding domain (LBD). The LBD folds into a canonical three-layer helical sandwich which contains a pocket for ligand binding (LBP) and the AF-2 domain involved in cofactors recruitment. The high sequence similarity among the four oSR LBDs explains certain promiscuity among ligands, able to bind to more than one receptor. In this sense, it has been shown that progesterone also exhibits a high affinity to MR and, as it only confers a weak MR transactivation activity, it is an antagonist of aldosterone action (antimineralocorticoid).[10–12] Remarkably, this promiscuity, also termed cross-reactivity, would be involved in several physiological disorders. For example, progesterone is suspected to exacerbate mineralocorticoid deficiency in patients with congenital adrenal hyperplasia by antagonism at the MR.[12,13] On the other hand, it is known that the S810L mutation within the human MR (MR S810L) switches progesterone from MR antagonist to MR agonist and subsequently, pregnancies carrying on this MR mutation suffer severe hypertension by MR activation.[14,15]

* Corresponding author. Fax: +54 11 4576 3385.
E-mail address: burton@qo.fcen.uba.ar (G. Burton).

0968-0896/$ - see front matter © 2011 Elsevier Ltd. All rights reserved.
doi:10.1016/j.bmc.2011.01.033

Numerous crystal structures of oSR LBD–steroid complexes have been obtained, showing that steroids are completely buried into a mainly hydrophobic ligand binding pocket (LBP) inside the globular protein structure.[16–19] Nevertheless, the oSR LBPs also contain some specific polar residues which interact with the ligand's oxygen atoms, establishing polar interactions essential to ligand–receptor recognition. Particularly, a canonical theme exists for recognition of the C3-carbonyl (C3O) group in the A-ring. The Δ^4-3-keto functionality of steroid hormones gives rise to a ring A conformation that allows an adequate interaction between the C3O and conserved residues of arginine and glutamine in the oSR. In the case of progesterone, the PR LBD–progesterone crystal structure (pdb:1a28, chain A) shows that the C3O participates in a polar interaction network that involves the Gln725, Arg766 and Met759 residues and a water molecule (Fig. 1). Several hydrogen bonds are formed among the C3O oxygen atom involving the N1H and N2H nitrogen atoms of the Arg766 guanidinium group, the NE2 nitrogen and the OE1 oxygen atoms of the Gln725 amide group and the water molecule. The water molecule occupies a small cavity between the steroid and receptor atoms interacting with the Gln725 and Arg766 side chains and the Met759 backbone carbonyl. In this way, the water molecule plays a fundamental role stabilizing the Gln725 and Arg766 interaction with the steroid C3O. In addition, the Arg766 NE nitrogen atom and the Tyr777 backbone oxygen also take part of this hydrogen bonding network around the progesterone A-ring, stabilizing the Arg766 conformation. It should be noted that although the progesterone binding mode observed in chain B of the same crystal structure (pdb:1a28) is very similar to that of chain A, the position of the NE2 nitrogen and the OE1 oxygen atoms of the Gln725 amide group appear inverted. Since the Gln amide assignment is a common problem in X-ray structure refinement with error rate well documented,[20] rotamer assignment of Gln725 in the PR LBD should be taken with caution.

Since the C3O relative position depends on the global steroid conformation, detailed structure–activity studies of steroids containing subset modifications in ring A may shed light in understanding the molecular basis involved in this ligand–receptor recognition. Compounds **2** and **3** were prepared as intermediates in the synthesis of A-homo analogues of the neuroactive steroids.[21] In that work, we found that the additional carbon atom combined with the Δ^5 double bond, resulted in a more flexible ring A.[21] The availability of the A-homo steroids **2** and **3** structurally related to progesterone, led us to evaluate how the A-ring flexibility affected the activity on PR and MR. Particularly, the transactivation activity of these compounds was evaluated and interestingly, we found that both A-homo compounds act as selective PR agonists but lack MR activity. In this work we investigate the biological activity of these compounds and use a set of computational methods to perform an in depth analysis of the conformations of both A-homo analogues and their putative interactions with the PR LBP, thus providing a molecular basis for the observed differences in biological activity.

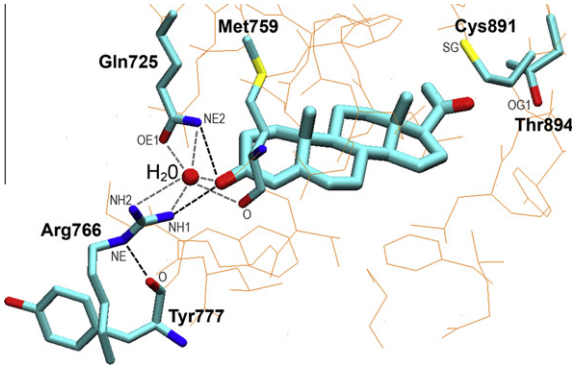

Figure 1. Ligand binding mode of progesterone (**1**) in the PR LBD–progesterone crystal structure (pdb:1a28, chain A). The C3-carbonyl ligand group participates in a hydrogen bonding network that involves the Gln725, Arg766 and Met759 residues and a water molecule. Dotted lines indicate distances between heavy atoms smaller than 3.5 Å. Polar residues around the C20-carbonyl are also shown.

2. Results

2.1. Biological activity of A-homo analogues

To evaluate the activity of compounds **2** and **3** on the PR and MR, Cos-1 cells were co-transfected with an expression vector codifying the luciferase reporter gene under the control of the Mouse Mammary Tumor Virus promoter (MMTV) and the vectors expressing the corresponding receptor.[22] Figure 2a shows that both A-homo analogues exhibited significant progestagen activity when they were administered at concentrations of 10^{-6} and 10^{-5} M. However, at variance with progesterone, the A-homo analogues did not exhibit mineralocorticoid or antimineralocorticoid responses (Supplementary data, Fig. S1). These results indicate that introduction of an additional carbon in ring A combined with a Δ^5 double bond, produces compounds able to act selectively on the PR. Moreover, results also show that at high concentrations (10^{-5} M) compound **3** is more active than compound **2**.

To further characterize in vitro the biological activity of the A-homo progesterone analogues, the transcription level of the anti-apoptotic isoform of the bcl-x gene was next evaluated in breast cancer mammary epithelial cells T47D. The bcl-x gene is alternatively spliced to produce at least two distinct mRNAs and two

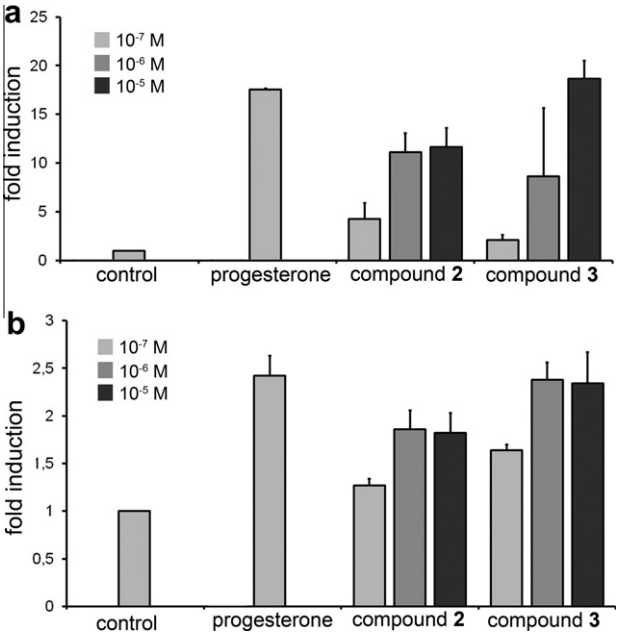

Figure 2. Progestagen activity of A-homo analogues **2** and **3**. Progesterone 10^{-7} M was used as positive control. (a) PR transactivation activity was evaluated using Cos-1 cells co-transfected with 1 μg of ph-*h*PRβ vector, 3 μg of pMMTV-Luc reporter vector and 1 μg of pCMV-LacZ vector. Cells were incubated for 24 h as indicated and luciferase activity was measured. After correcting for β-galactosidase activity, the values are expressed as fold induction relative to the control (untreated cells). The means ± SE from three independent experiments are shown. (b) Bcl-xL expression was evaluated in T47D cells incubated for 6 h as indicated. The RNA was extracted and quantified by qPCR. Values are expressed as fold induction relative to the control (untreated cells). The means ± SE from three independent experiments are shown.

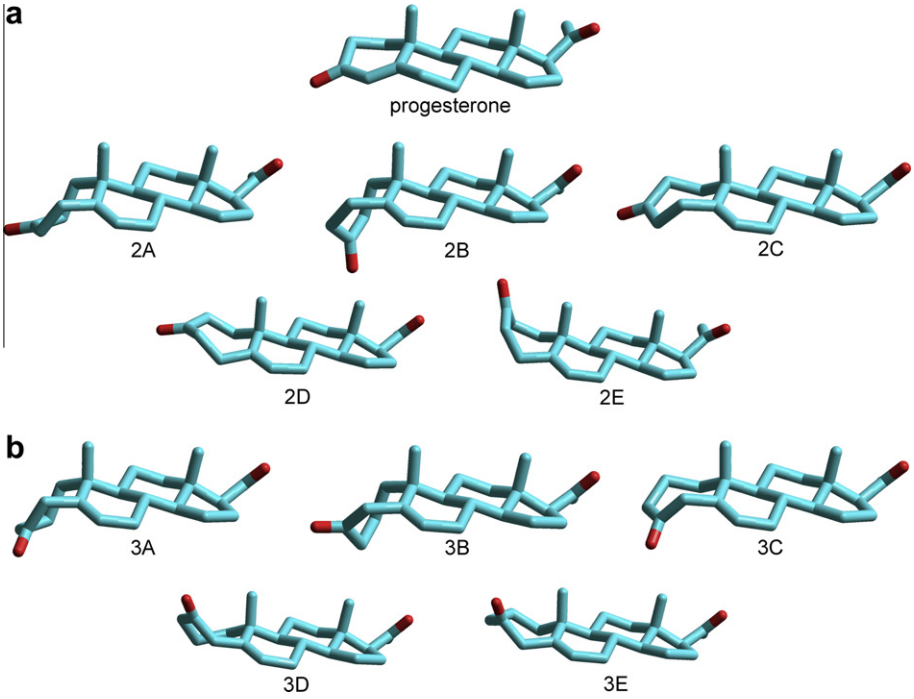

Figure 3. Calculated HF/6-31G** conformers of compounds **2** (a) and **3** (b). The HF/6-31G** optimized structure of progesterone (**1**) is shown at the top for comparison.

variant proteins which have antagonistic functions; the longer one (Bcl-xL) inhibits apoptosis, whereas the shorter one (Bcl-xS) activates it.[23] Bcl-xL is highly expressed in many types of cancers including breast cancer and has been associated with an increased risk of metastasis in this disease.[24] Bcl-xL expression has been previously demonstrated to be progesterone and glucocorticoid dependent.[25] Results presented here show that both compounds **2** and **3** have a significant progestagen activity (Fig. 2b), being the activity of compound **3** again higher than the activity of compound **2**. In fact, the efficacy of compound **3** at 10^{-6} M is similar to that observed with progesterone at 10^{-7} M.

2.2. Conformational analysis of A-homo analogues

In the A-homo analogues **2** and **3**, the higher conformational mobility of the seven-membered A-ring combined with an enhanced flexibility at the A/B ring junction introduced by the 5,6 double bond in ring B, allow these steroids to explore several conformations. Semiempirical AM1 geometry optimizations starting from different initial structures of compounds **2** and **3** gave five energy minima for each compound. These were further optimized using HF/6-31G**, to give the corresponding ab initio conformers shown in Figure 3. Table 1 shows the values for torsion angles C19–C10–C1–C2 (*T*1), C6–C5–C4a–C4 (*T*2) and C1–C2–C3–C4 (*T*3) or C2–C3–C4–C4a (*T*3′) used to characterize the ring A conformation of each conformer and the HF/6-31G** relative energies. For both compounds two distinct groups are evident, three low energy conformers (dubbed **A**, **B**, **C**) within less than 2 kcal/mol of the most stable conformer and two higher energy conformers(dubbed **D**, **E**) differing by more than 5 kcal/mol from that conformer.

The low energy conformers of compound **2** (**2A**, **2B** and **2C**) have similar *T*2 values corresponding to a 4α,4aβ arrangement. In contrast, the 4β,4aα arrangement of conformers **2D** and **2E** leads to an A-ring torsioned towards the β face that presents steric repulsion with the C19 methyl group, resulting in less stable structures. Conformers **2A** and **2B** have a 1β,2α arrangement (similar *T*1), but differ in the relative position of the C3 (*T*3), which determines the carbonyl orientation. The C3O of conformer **2B** is oriented perpendicularly to the steroid nucleus plane, leading to a torsioned and slightly less stable global conformation. The **2C** conformer has a flat global structure with a 1α,2β arrangement but almost the same energy as **2B**. Similar results were obtained with compound **3**; thus, the 4α,4aβ arrangement (similar *T*2) corresponds to the more stable conformers **3A**, **3B** and **3C** while the β-torsioned structures (**3D** and **3E**, 4β,4aα arrangement) are less stable. Again, conformers **3A** and **3B** only differ from each other in the C3 carbonyl orientation (*T*3′), although the energy difference (0.8 kcal/mol) is smaller than in the case of the **2A** and **2B** conformers (1.21 kcal/mol). As in compound **2**, the 1α,2β arrangement of conformer **3C** gives a slightly less stable flat conformation.

Table 1
Ring A torsion angle values and relative energy of conformers of compound **2** and **3** from HF/6-31G** calculations[a]

Conformer	Torsion angle[b] (°)				ΔE_g[c] (kcal/mol)	ΔE_{aq}[d] (kcal/mol)
	*T*1	*T*2	*T*3	*T*3′		
2A	−173	−97	−57	—	0.00	0.00
2B	−171	−102	29	—	1.21	0.96
2C	−52	−104	42	—	1.29	1.05
2D	−38	137	51	—	5.74	5.68
2E	−55	130	−68	—	6.63	6.46
3A	−159	−86	—	48	0.00	0.00
3B	−174	−107	—	−73	0.76	0.74
3C	−56	−103	—	23	1.62	1.46
3D	−32	152	—	−74	5.25	5.48
3E	−87	155	—	−6	7.44	7.46

[a] See Figure 3 for 3D structures of individual conformers.
[b] *T*1 (C19–C10–C1–C2), describes the orientation of carbon C2 (relative to the steroid nucleus plane). *T*2 (C6–C5–C4a–C4) describes the orientation of carbon C4. *T*3 (C1–C2–C3–C4) and *T*3′ (C2–C3–C4–C4a) depict the orientation of the C3O or C4-carbonyl (C4O) groups in compounds **2** and **3**, respectively.
[c] Gas phase energy difference relative to the most stable conformer (**2A** for compound **2** and **3A** for compound **3**).
[d] Energy difference in aqueous solution (from IEFPCM calculations) relative to the most stable conformer (**2A** for compound **2** and **3A** for compound **3**).

Since three stable conformers with comparable energies were predicted for each compound, it is possible to assume that an equilibrium mixture containing significant proportions of all three conformers would exist at room temperature. To evaluate the dynamic behavior of both compounds **2** and **3**, 1 ns AM1-MD simulations were performed taking each stable conformer as initial structure. This study showed that the **2A** and **2B** conformers exchange by modifying the C3O orientation (data not shown) with the **2A** conformer being favored due to its lower relative energy. In contrast, no exchange was observed between the **3A** and **3B** conformers, which remained in their original conformations during the time-scale of the simulation. Thus, although the energy difference between the **3A** and **3B** conformers is only 0.8 kcal/mol, the energy barrier of interconversion is probably too large to achieve this conformational change in the conditions of the simulation. Both **2C** and **3C** conformers also remained in their original conformation during the entire trajectory. Finally, to further characterize the dynamical behavior of each conformer, 10 ns of Amber-MD simulations were carried out using an explicit TIP3P water box as solvent model. The dynamic behavior of all conformers was similar to that obtained in the AM1-MD simulations.

2.3. Ligand binding mode of A-homo analogues in the progesterone receptor (PR)

To study the molecular basis of the interaction between the A-homo analogues **2** and **3** and the PR ligand binding pocket (PR LBP), Amber-MD simulations of PR LBD-**2** and PR LBD-**3** complexes were performed. The PR LBD–progesterone crystal structure (pdb:1a28, chain A),[18] was used as initial structure and the PR LBD–progesterone MD simulation was performed as a control trajectory. All the simulated complexes were constructed by removing the crystallized water molecules and immersing the protein and ligand atoms in a box of explicit water molecules (see Material and Methods). No water molecules occupying the cavity around the A-ring carbonyl were present in any of the initial complexes (compare with Fig. 1).

2.3.1. PR LBD–progesterone complex

During the equilibration steps of the PR LBD–progesterone simulation (See Material and Methods) we observed that a water molecule rapidly moved into the cavity around the C3O, occupying a position similar to that in the PR LBD–progesterone crystal structure (see Fig. 1). This water molecule remained in that position throughout the 10 ns of the trajectory. Figure 4a shows a representative snapshot of the progesterone binding mode observed in the MD simulation. As expected, the interaction between the C3-carbonyl and both Arg766 N1H and Gln725 NE2, remained stable during the time-scale of the simulation (Fig. 4b) with average values of 3.30 and 3.36 Å, respectively. The water molecule is not in a fixed position, but moves inside the cavity by forming and breaking several hydrogen bonds with the surrounding nitrogen and oxygen atoms. The schematic representation of this hydrogen bonding network (Supplementary data, Fig. S2) shows that all polar interactions are formed with high frequency and that the water molecule interacts with the ligand during almost half of the simulation. Similar results about the progesterone binding mode were obtained by Hillisch et al. performing a 4 ns MD simulation of the PR LBD–progesterone complex.[26] The above results from MD simulations are thus in agreement with the binding mode observed in the crystal structure (pdb:1a28). However, the preferred Gln725 rotamer observed in the MD simulation is opposite to the rotamer assigned in the chain A used here as initial structure, although equal to the rotamer observed in the chain B. In order to confirm that the Gln725 rotamer obtained in the MD simulation produced a more stable hydrogen bond network, we used the NQ-Flipper program, a web service based on mean force potentials to automatically detect and correct erroneous Asn and Gln rotamers.[27] In agreement with the MD results, the NQ-Flipper program revealed that in chain B the Gln725 rotamer was correctly assigned, while in chain A the assignment of the Gln725 amide group was reversed.

2.3.2. PR LBD-2 complex

In silico PR LBD-**2A**, PR LBD-**2B** and PR LBD-**2C** complexes were constructed by superimposing the C ring carbon atoms of the A-homo steroid with the equivalent atoms of progesterone in the crystal structure (See Material and Methods). During the equilibration step conformers **2A** and **2C** remained in their original conformation within the PR LBP, while the **2B** conformer evolved to the **2A** conformation. Thus the PR LBD-**2B** complex was discarded and only the PR LBD-**2A** and PR LBD-**2C** systems were further analyzed.

A representative snapshot of the **2A** binding mode is shown in Figure 5a. Visual inspection of the PR LBD-**2A** trajectory clearly shows that during the simulation the side chain of Arg766 rotates away from the C3-carbonyl position. The evolution of the distance between the oxygen atom of the C3-carbonyl and the N1 nitrogen atom of Arg766 reveals this behavior (Fig. 5b). The Arg766 side chain rotation is highly correlated with the loss of interaction with the carbonyl backbone of Tyr777 and causes an expansion of the cavity around the C3-carbonyl allowing the entry of several exchangeable water molecules. In fact, 14 different water mole-

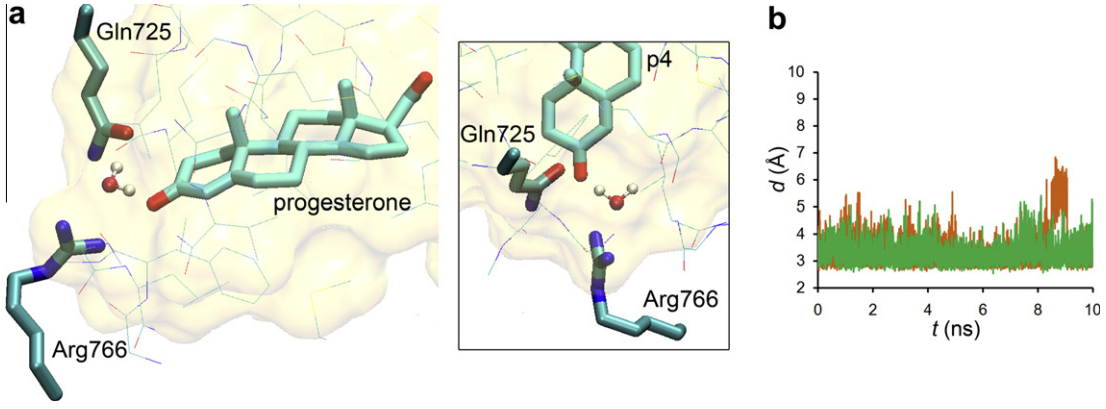

Figure 4. (a) Representative snapshot of the ligand binding mode of progesterone (**1**) during the MD simulation. The box area shows a view perpendicular to the steroid skeleton. (b) Time evolution of the distance (*d*) between the C3O oxygen atom of progesterone and the N1H nitrogen atom of Arg766 guanidinium group (green) or the NE2 nitrogen atom of Gln725 amide group (orange).

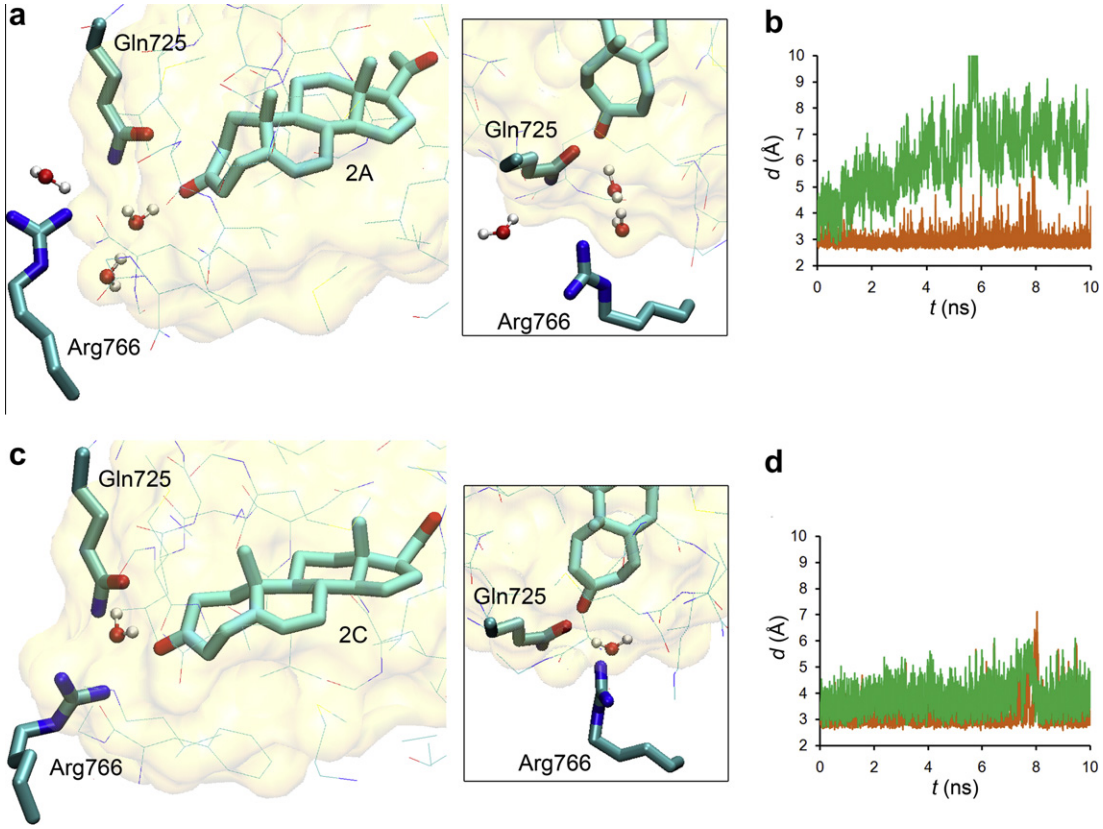

Figure 5. (a) Representative snapshot of the ligand binding mode of conformer **2A** during the MD simulation. The box shows a view perpendicular to the steroid skeleton. (b) Time evolution of the distance between the C3O oxygen atom of conformer **2A** and the N1H nitrogen atom of Arg766 guanidinium group (green) or the NE2 nitrogen atom of Gln725 amide group (orange). (c) Representative snapshot of the ligand binding mode of conformer **2C** during the MD simulation. The box shows a view perpendicular to the steroid skeleton. (d) Time evolution of the distance between the C3O oxygen atom of conformer **2C** and the N1H nitrogen atom of Arg766 guanidinium group (green) or the NE2 nitrogen atom of Gln725 amide group (orange).

cules were found closer than 3.5 Å from the C3-carbonyl oxygen throughout the simulation. Thus, the α-torsioned conformation of **2A** prevented an adequate Arg766 orientation impeding the formation of the hydrogen bonding network around the A ring, fundamental for the C3-carbonyl recognition. In view of this behavior, we may conclude that the **2A** conformer is unable to properly interact with the PR LBP.

At variance with the above, the binding mode of conformer **2C** was similar to that observed in the PR LBD–progesterone complex (Fig. 5c). The hydrogen bonds between the C3O and both Arg766 N1H and Gln725 NE2 remained stable during the 10 ns of the simulation (Fig. 5d), with average values of 3.83 and 3.10 Å, respectively. As in the previous case, the Gln725 amide rotated acquiring a similar disposition to that in the PR LBD–progesterone complex and a water molecule occupied the corresponding cavity completing the hydrogen bonding network. However, this water molecule did not enter at the equilibration step as in the case of the PR LBD–progesterone, but after 1 ns. The schematic representation of the polar interactions revealed that the hydrogen bonds are not as frequent as those observed for the progesterone complex (Supplementary data, Fig. S2b). Thus, using MD simulation we found that in the case of compound **2** it is not the more stable conformer **2A**, but the less stable conformer **2C** the one that has a binding mode similar to that of progesterone, although with a less efficient hydrogen bonding network.

2.3.3. PR LBD-3 complex

In silico PR LBD-**3** complexes were constructed similarly to the PR LBD-**2** complexes (See Material and Methods). During the equilibration step the steroid molecules in the PR LBD-**3B** and PR LBD-**3C** complexes remained in their original conformation, while the **3A** conformer evolved into **3B**. Thus, only PR LBD-**3B** and PR LBD-**3C** systems were further analyzed.

Results obtained with the PR LBD-**3B** complex showed that the **3B** conformer is bound into the LBP of PR LBD (Fig. 6a) in a similar way as progesterone. The Gln725 amide group rotated to give the preferred rotamer, and a water molecule occupied the cavity in the equilibration step and remained there throughout the simulation. Notably, the interactions between the C4O and both Arg766 N1H and Gln725 NE2 were stronger than in the PR LBD–progesterone complex, with average distances of 3.24 and 3.07 Å, respectively (Fig. 6b). The rest of the hydrogen bonds also formed at higher frequency than in the progesterone system (Fig. S2c). Hence, the LBP of the PR LBD had the ability to accommodate the A-ring conformation of the **3B** conformer, forming the hydrogen bonding network around the C4O required for ligand recognition.

In the case of the **3C** conformer, a conformational change of the Gln725 side chain occurred during the MD simulation (Fig. 6c). As shown in Figure 6d, the Gln725 rotation occurred at the beginning of the simulation and caused an expansion of the cavity, allowing the entry of two water molecules instead of one (Fig. 6d). Thus, in contrast to compound **2**, the MD results obtained show that in the case of compound **3** the more stable conformer **3B** results in a ligand binding mode similar to that of progesterone.

2.3.4. C20-carbonyl polar interactions

According to the PR LBD–progesterone crystal structure (Fig. 1), there are two residues, Cys891 and Thr894, that may form hydro-

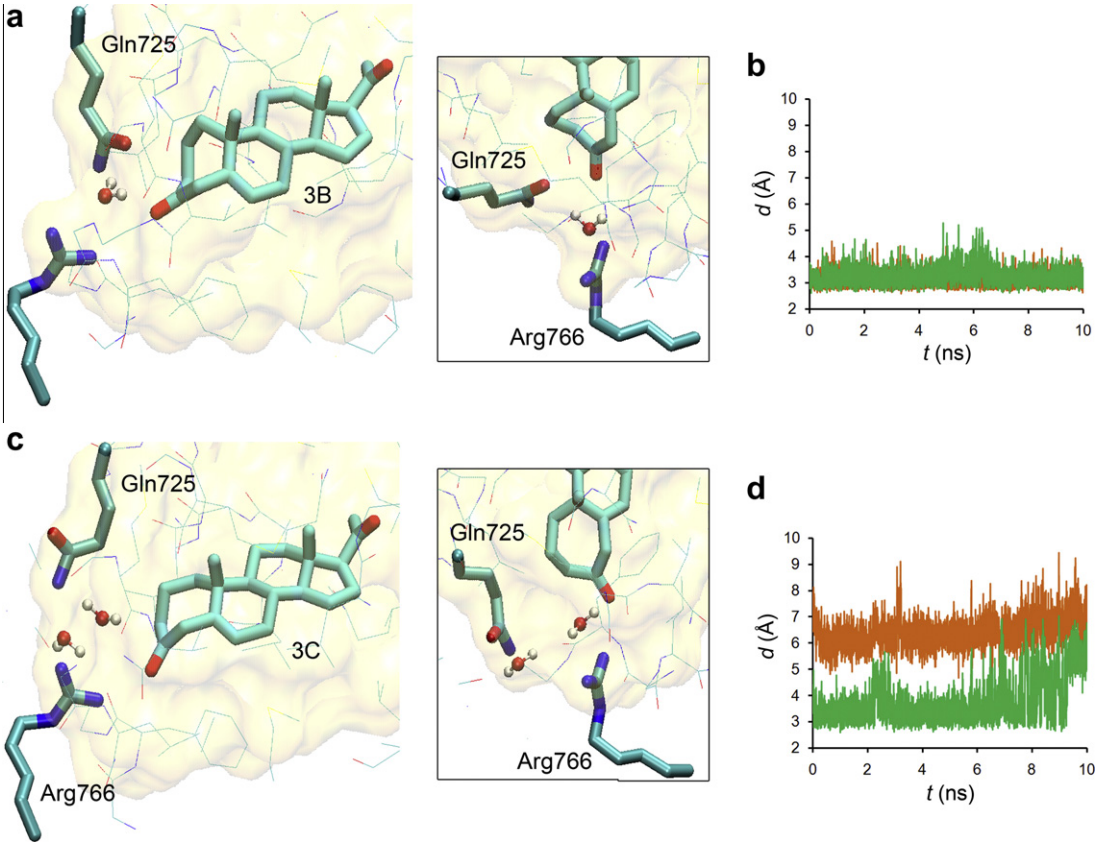

Figure 6. (a) Representative snapshot of the ligand binding mode of conformer **3B** during the MD simulation. The box shows a view perpendicular to the steroid skeleton. (b) Time evolution of the distance between the C3O oxygen atom of conformer **3B** and the N1H nitrogen atom of Arg766 guanidinium group (green) or the NE2 nitrogen atom of Gln725 amide group (orange). (c) Representative snapshot of the ligand binding mode of conformer **3C** during the MD simulation. The box shows a view perpendicular to the steroid skeleton. (d) Time evolution of the distance between the C3O oxygen atom of conformer **3C** and the N1H nitrogen atom of Arg766 guanidinium group (green) or the NE2 nitrogen atom of Gln725 amide group (orange).

gen bonds with the C20O. The MD results show that the C20O of progesterone and of both A-homo analogues did not form stable polar interaction with these residues. As shown in Table S1, the frequency of hydrogen bond formation in all cases is less than 30%, suggesting that the C20-carbonyl may not be playing a critical role for PR recognition and transactivation. Similar conclusions were proposed previously by Hillisch et al. from their PR LBD–progesterone MD simulation.[26] Nevertheless, it should be noted that conformer **3B** has an equivalent frequency of hydrogen bond formation for its C20O oxygen compared to progesterone if both Cys891 and Thr894 are taken together.

2.4. Energy contributions to PR LBD–steroid binding

In order to evaluate the different contributions to the binding energy between the PR LBD and progesterone and the A-homo steroids presented above, we applied the MM-GBSA method as implemented in AMBER9. Particularly, we were interested in the comparison of electrostatic (ele) and van der Waals (vdw) protein–steroid interaction energies as computed by the molecular mechanics force field (MM) in each complex. Moreover, we also estimated the total binding free energy (ΔG) by incorporating solvation contribution terms using the Generalized Born (GBSA) method. It should be noted that the estimated free energy does not include entropy changes in neither the protein nor the ligand, thus it should be used only for comparative purposes.

First we applied the MM-GBSA method without considering the water molecule involved in the polar network around the A-ring carbonyl ($\Delta_{LBD-ligand}$, Table 2). Consistent with the previous hydrogen bond analysis with both Arg766 and Gln725 residues, electrostatic interaction is higher for the progesterone, **2C** and **3B** systems compared with the **2A** and **3C** complexes. Remarkably, although hydrogen bond frequencies were larger in the presence of **3B** compared to progesterone (Supplementary data, Fig. S2), the electrostatic interaction resulted most favorable in the progesterone complex. As expected for this type of hydrophobic ligands, in all cases the vdw contribution is dominant. Interestingly, all A-homo conformers have a bigger vdw interaction than progesterone, probably due to the increase of the nonpolar surface produced by the additional carbon atom in the A-ring. The total MM energy (ele + vdw) also shows more favorable interactions in the progesterone, **2C** and **3B** systems compared to the **2A** and **3C** complexes. When the solvation terms were included (ΔG), the order of relative energies changed slightly and the values were closer for all the complexes. Thus the energy analysis clearly reveals the conformational preference of **2C** and **3B** over **2A** and **3C**, and an increase in vdw interaction for the A-homo steroids compared to the natural progesterone molecule.

Finally, in view of the possible essential role played by the trapped water molecule described previously, we computed the interaction energies for the progesterone, **2C** and **3B** complexes but including the water molecule explicitly either as part of the receptor ($\Delta_{LBDW-ligand}$, Table 2) or as part of the ligand ($\Delta_{LBD-ligandW}$, Table 2). The results show that including the water as part of the receptor gives only a minor contribution to the interaction energy, the values being actually slightly smaller than those without the water molecule but with the same trends. On the other hand, by including the water as part of the ligand a significant increase of

Table 2
Interaction energy contributions (MM-GBSA) of PR-LBD complexes with relevant conformers of **2** and **3**[a]

	$\Delta_{LBD-ligand}$[b] (kcal/mol)					$\Delta_{LBDW-ligand}$[c] (kcal/mol)			$\Delta_{LBD-ligandW}$[d] (kcal/mol)		
	1	**2C**	**3B**	**2A**	**3C**	**1**	**2C**	**3B**	**1**	**2C**	**3B**
ele	−23.3	−17.1	−16.8	−10.2	−10.4	−21.5	−15.9	−15.9	−51.8	−44.5	−44.7
vdw	−50.4	−53.6	−54.7	−53.5	−50.9	−51.5	−54.0	−55.0	−49.0	−51.0	−52.0
MM	−73.7	−70.8	−71.5	−63.7	−61.3	−73.0	−69.9	−70.9	−100.8	−95.5	−96.7
ΔG	−45.9	−46.9	−48.0	−45.6	−40.5	−46.8	−47.8	−49.0	−53.7	−54.2	−55.6

[a] ele = electrostatic energy, vdw = van der Waals energy, MM = ele + vdw (total molecular mechanics energy), ΔG = total binding free energy estimating the solvation energies with the Generalized Born method.
[b] $\Delta_{LBD-ligand}$: protein–ligand interaction energies.
[c] $\Delta_{LBDW-ligand}$: protein–ligand interaction energy including the trapped water molecule as part of the receptor.
[d] $\Delta_{LBD-ligandW}$: protein–ligand interaction energies including the trapped water molecule as part of the ligand.

the electrostatic energy was obtained. This result shows that the trapped water strongly interacts with the protein and may be considered a structural water, it is expected to contribute to the overall binding since it is bound together with the ligands. In both cases the total MM energy reveals that the largest binding interaction occurred with progesterone, followed by **3B** and then **2C**. The difference between the **2C** and **3B** conformers resides mainly in the larger vdw interaction of **3B** with the PR LBP.

3. Discussion

Progesterone is one of the most relevant steroid hormones in humans. Its classical mode of action involves the nuclear receptor PR, although in recent years several other non-genomic mechanisms of action have been found, including binding to the membrane receptor PR and rapid actions over the CNS.[28–30] Regarding the oSR, it is well known that polar interactions play a fundamental role in both binding and receptor activation. Upon interaction with two conserved residues (arginine on helix 5 and glutamine on helix 3) and a water molecule, the steroid C3-carbonyl forms a stable polar interaction which recognizes and maintains the steroid properly oriented. In the MR, it has been proposed that formation of this hydrogen network would be involved in the bending of helix 3 towards helix 5, a structural requirement for receptor activation.[31] This conserved mechanism might be extended to the other members the oSR family, therefore a precise understanding of its molecular basis is required to understand both ligand recognition and receptor activation. In this sense, although X-ray structures and docking studies give valuable information on the molecular determinants of steroid action, the study of the dynamic behavior is essential to improve our knowledge of receptor–ligand systems. MD simulation is a widely employed tool to provide this information, since it considers the inherent flexibility of both receptor and ligand molecules.

In this work, we evaluated the PR and MR activities of two A-homo analogues of progesterone (**2** and **3**) which differ only in the position of the A-ring carbonyl. Both compounds acted as selective PR agonists, with compound **3** being more active than **2**. Semiempirical and ab initio methods evidenced three low energy conformers for each A-homo steroid, two of which differ only in the carbonyl orientation (**2A**/**2B** and **3A**/**3B**). Analysis of the binding modes of all conformers in the PR LBD using 10 ns MD simulations showed that conformers **2B** and **3A** rapidly changed the C3 carbonyl orientation evolving to **2A** and **3B**, respectively. Furthermore compounds **2** and **3** have only one conformer (**2C** and **3B**) able to properly form the hydrogen bonding network with Arg766 and Gln725. The **2C** and **3B** ligand binding modes were similar to that of progesterone, with hydrogen bond frequencies even larger in the presence of **3B**. In contrast, **2A** and **3C** appear unable to interact adequately with the PR LBD: while **2A** led to the rotation of the Arg766 side chain, **3C** caused the rotation of the Gln725 side chain. The superposition of HF/6-31G** optimized

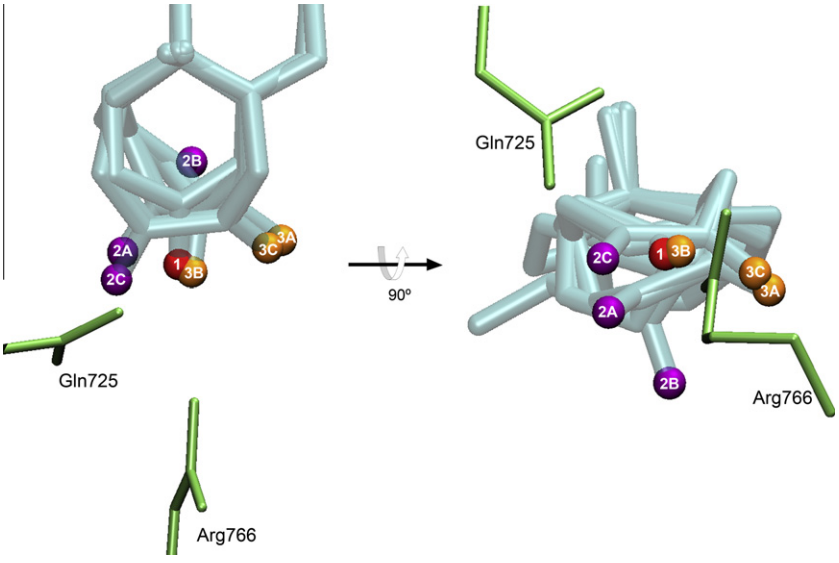

Figure 7. Top (left) and front (right) view of the superposition of HF/6-31G** most stable conformers of compound **2** (**2A**, **2B** and **2C**) and **3** (**3A**, **3B** and **3C**) with the progesterone structure in the PR LBD–progesterone crystal structure (pdb:1a28). The position of the C3O oxygen atom of progesterone is shown in red, the position of the C3O oxygen atoms of the conformers of **2** are shown in violet and the position of the C4O oxygen atoms of the conformers of **3** are shown in orange.

structures of these conformers with the progesterone structure as found within the crystal structure of the PR LBD–progesterone complex, may be used to explain the different ligand binding modes obtained for each A-homo conformer. As shown in Figure 7, the oxygen atom closest to the position of the progesterone C3-carbonyl oxygen corresponds to the C3O in conformer **3B**, in agreement with the ability of this conformer to strongly interact with both Arg766 and Gln725. In contrast, the carbonyl oxygen in the **3C** conformer is displaced towards the Arg766 position, resulting in a distance to Gln725 too large to form a hydrogen bond. In the case of compound **2** instead, oxygen atoms in both **2A** and **2C** conformers are oriented towards the Gln725. However in the **2A** conformer the distance to the Arg766 is larger than in **2C** conformer, supporting the lack of a hydrogen bond between **2A** and this residue.

Computational methods show that both compounds **2** and **3** have one conformer that may be recognized by the PR, in agreement with the observed progestagen activity. The difference between the A-homo compounds might explain the fact that compound **3** results more active than **2**. While the **3** conformer able to bind is the most stable, in the case of **2** the conformer that is able to bind is the less stable. Moreover, compound **3** has two stable conformers that end in optimal ligand binding, while compound **2** has only one. Thus, the larger population of **3** conformers that may be recognized by the receptor would explain the higher activity of this A-homo steroid. Analysis of the energy contributions involved in each steroid–receptor interaction showed that although the van der Waals energies are the larger components for all complexes, the main variations are found in the electrical components. The higher interaction energy when the water molecule is considered as part of the ligand has also interesting implications; mimicking this water molecule by properly positioned functional groups could result in high affinity ligands by reducing the entropy loss due to the trapped molecule.

Although the molecular determinants of the inability of A-homo steroids **2** and **3** to induce transactivation on the MR have not been established, this may reside in part in the larger hydrophobic surface of these compounds compared to progesterone. The only difference between the LBPs of the PR and MR receptors in the region surrounding the steroid A ring, is the replacement of the nonpolar Met759 in PR (see Fig. 1) by a polar Ser810 in MR. Consequently, the larger nonpolar surface of compounds **2** and **3** in the vicinity of a more polar receptor surface may destabilize the ligand–receptor interaction and hamper the A-homo steroid binding, thus explaining the lack of MR activity.

The above findings indicate that steroidal and non-steroidal compounds that may adopt the global conformation of the A-homo analogues, especially that of compound **3**, may lead to novel selective PR modulators. Moreover, A-homo analogues of other steroid hormones may prove useful to investigate structure–activity relationships and in the search for novel oSR selective ligands.

4. Experimental section

4.1. Biological activity

4.1.1. Steroids

A-homo-5-pregnene-3,20-dione (**2**) and A-homo-5-pregnene-4,20-dione (**3**) were prepared as described previously (see Supplementary data for spectral data).[21] Progesterone and aldosterone were from Sigma Co. (St. Louis, MO).

4.1.2. Transactivation activity

Cos-1 cells were cultured at 37 °C under humidified atmosphere with 5% CO_2 in DMEM supplemented with 10% fetal calf serum (FCS) containing penicillin (100 IU/mL), streptomycin (100 mg/mL) and glutamine (2 mM) in p100 plates. For transient transfections, 5×10^5 cells were plated in 60 mm plates and transfected with lipofectin according to the manufacturer protocol (Lipofectine Plus, Gibco, Inc.). Analyses of PR activity were performed by transfecting 3 μg of pMMTV-Luc plasmid which expresses luciferase enzyme under the control of Mouse Mammary Tumor Virus promoter containing several hormone receptor elements (HRE),[32] 1 μg phPR expressing human isoform B of the progesterone receptor[33] and 3 μg of pRSV-LacZ (Clontech Inc., Palo Alto, CA) as control of transfection. After (18 h) transfection, the medium was replaced by new one containing 10% charcoal-stripped CS and antibiotics. Cells were then incubated during 24 h with steroids at the concentrations indicated. Steroids were applied from 1000-fold stock solutions in dimethylsulfoxide. Incubations were stopped by aspirating the medium and washing the cells twice with phosphate buffered saline (PBS). Cells were then harvested in lysis buffer and luciferase activity was measured according to the manufacturer protocol (Promega Inc.). Galactosidase activity was measured as previously described.[34] Analyses of the MR activity were performed in a similar way using 1 μg of phMR plasmid which expresses the human mineralocorticoid receptor.

4.1.3. Bcl-x_L expression levels by RNA analysis

T47D cells were cultured at 37 °C under humidified atmosphere with 5% CO_2 in RPMI 1640 medium plus 10% fetal calf serum and 1% penicillin/streptomycin in p100 plates. Cells (5×10^5) were plated in p60 plates with medium containing 10% charcoal-stripped CS and antibiotics and treated with progesterone or with the A-homo analogues at the concentrations indicated during 6 h. RNA was extracted with Trizol reagent according to the manufacturer instructions (Invitrogen, USA). For reverse transcription, 1 μg of total RNA was used. The first cDNA strand was synthesized with 200U MMLV reverse transcriptase (Promega, Madison, WI, USA); 25 ng/l random primers (Invitrogen, USA); 2 g/l Rnasin (Promega, Madison, WI, USA) and 1.5 mM dNTPs (Invitrogen, USA). Retrotranscription was performed at 37 °C for 60 min followed by 5 min at 72 °C. For quantitative real-time polymerase chain reaction (qPCR), an aliquot of 0.2 μl cDNA was used. All reactions were conducted in a volume of 25 μl containing 4 mM $MgCl_2$ (Invitrogen, USA), 0.2 mM dNTPs (Invitrogen, USA), 0.75U Taq polymerase (Invitrogen), 1/30000 Sybr Green (Roche) and specific oligonucleotides for bcl-xL gene forward: 5′-GGTATTGGTGAGTCGGATCG-3′ and reverse: 5′-TTCCACAAAAGTATCCCAGC-3′ in a DNA Engine Opticon instrument (MJ Research). Reactions were run for 35 cycles under the following conditions: 15 s at 94 °C, 20 s at 66 °C and 25 s at 72 °C. The amplification of unique products in each reaction was verified by melting curve and Ethidium Bromide (Sigma Aldrich) stained 2% agarose gel electrophoresis. bcl-X_L expression level was normalized to gapdh expression by qRT-PCR performed with specific oligonucleotides (forward: 5′-TTGATTTTGGAGGGATCTCG-3′ and reverse: 5′-GAGTCAACGGATTTGGTCGT-3′) by using standard curve method. Means and standard errors from at least three experiments were calculated and shown as fold changes respect to control (untreated cells).

4.2. Computational methods

4.2.1. Semiempirical and quantum mechanics calculations

The geometries of compounds **2** and **3** were built in silico and optimized with the AM1 method using the HyperChem program (Hypercube). Following this initial rough optimization, these structures were further optimized using the HF method with the 6-31G** basis set in the quantum chemistry program GAUSSIAN 03.[35] Relative energies in aqueous media were estimated from single point IEFPCM calculations performed on the optimized geometries.

To build the corresponding force field parameters, RESP (restraint electrostatic potential) atomic partial charges were computed for the corresponding optimized structures (See Supplementary data for .mol files of all conformers).

4.2.2. Molecular dynamics

Molecular dynamics (MD) were performed by using the AMBER 9 software package.[36] The starting structure for the simulation was taken from the crystal structure of the PR LBD–progesterone complex (chain A of the pdb code:1a28).[18] The PR LBD-**2** and PR LBD-**3** complexes were built in silico, superimposing the C-ring carbon atoms of the A-homo steroid with the corresponding atoms of the progesterone molecule in the PR LBD–progesterone complex. The ligand parameters were assigned according to the general AMBER force field (GAFF) and the corresponding RESP charges using the Antechamber. The complexes were immersed in an octahedral box of TIP3P water molecules using the Leap module, giving final systems of around 30000 atoms. The systems were initially optimized and then gradually heated to a final temperature of 300 K. Starting from these equilibrated structures, MD production runs of 10 ns were performed for each system. All simulations were performed at 1 atm and 300 K, maintained with the Berendsen barostat and thermostat respectively,[37] using periodic boundary conditions and the particle mesh Ewald method (grid spacing of 1 Å) for treating long-range electrostatic interactions with a uniform neutralizing plasma. The SHAKE algorithm was used to keep bonds involving H atoms at their equilibrium length, allowing the use of a 2 fs time step for the integration of Newton's equations. The Amber99 force field parameters were used for all residues,[38] except for the ligands. Hydrogen bond populations were calculated as the percentage of snapshots where the H-bond was present. A H-bond was defined as present whenever the distance between both heavy atoms involved in the interaction was less than 3.5 Å (See Supplementary data Fig. S3, for the RMS profiles of MD simulations).

The AM1-MD simulation of A-homo conformers were performed with HyperChem 8.0 (Hypercube) taking the corresponding HF/6-31G** optimized geometries as starting structures. The simulations were performed in vacuo using a time step of 1 fs at constant temperature (300 K) maintained with a bath relaxation time of 0.1 ps.

4.2.3. MM-GBSA method

To compute interaction energy contributions the MM-GBSA method was applied as implemented in AMBER 9.[36] Calculations were performed on 400 snapshots of the last 8 ns of each PR LBD-ligand trajectory. Computed energetic contributions corresponded to the electrostatic energy (ele) and Van der Waals contributions (vdw) arising from bond, angle and dihedral terms in the force field, the sum of which gave the total gas phase binding energy (MM). Solvation free energy was estimated using the Generalized-Born approximation, which is based on the use of cavitation and electrostatic energy components. The total gas phase binding energy plus solvation free energy contribution gave the total binding free energy estimation (ΔG).

Acknowledgments

This work was supported by grants from Agencia Nacional de Promoción Científica y Tecnológica (PICT 00727), CONICET (PIP 0579) and Universidad de Buenos Aires (X026). Computational resources were provided by the 'Centro de Computación de Alto Rendimiento', FCEN-UBA. We thank Dr. Mario Galigniana (FIL-CONICET) for providing us with the phMR plasmid.

A. Supplementary data

Supplementary data associated with this article can be found, in the online version, at doi:10.1016/j.bmc.2011.01.033. These data include MOL files and InChiKeys of the most important compounds described in this article.

References and notes

1. DeMayo, F. J.; Zhao, B.; Takamoto, N.; Tsai, S. Y. *Ann. N.Y. Acad. Sci.* **2002**, *955*, 48.
2. Madauss, K. P.; Stewart, E. L.; Williams, S. P. *Med. Res. Rev.* **2007**, *27*, 374.
3. Schumacher, M.; Guennoun, R.; Robert, F.; Carelli, C.; Gago, N.; Ghoumari, A.; Gonzalez Deniselle, M. C.; Gonzalez, S. L.; Ibanez, C.; Labombarda, F.; Coirini, H.; Baulieu, E. E.; De Nicola, A. F. *Growth Horm. IGF Res.* **2004**, *14*, S18.
4. Hu, Z.; Li, Y.; Fang, M.; Wai, M. S.; Yew, D. T. *Curr. Med. Chem.* **2009**, *16*, 1418.
5. Lamb, R.; Harrison, H.; Clarke, R. B. *Ernst Schering Found Symp. Proc.* **2007**, 1.
6. Cutini, P. H.; Massheimer, V. L. *Steroids* **2010**, *75*, 355.
7. Scarpin, K. M.; Graham, J. D.; Mote, P. A.; Clarke, C. L. *Nucl. Recept. Signal* **2009**, *7*, e009.
8. Moore, J. T.; Collins, J. L.; Pearce, K. H. *ChemMedChem* **2006**, *1*, 504.
9. Gronemeyer, H.; Gustafsson, J. A.; Laudet, V. *Nat. Rev. Drug Disc.* **2004**, *3*, 950.
10. Myles, K.; Funder, J. W. *Am. J. Physiol. Endocrinol. Metab.* **1996**, *270*, E601.
11. Wambach, G.; Higgins, J. R. *Endocrinology* **1978**, *102*, 1686.
12. Quinkler, M.; Meyer, B.; Bumke-Vogt, C.; Grossmann, C.; Gruber, U.; Oelkers, W.; Diederich, S.; Bahr, V. *Eur. J. Endocrinol.* **2002**, *146*, 789.
13. Kuhnle, U.; Land, M.; Ulick, S. *J. Clin. Endocrinol. Metab.* **1986**, *62*, 934.
14. Geller, D. S.; Farhi, A.; Pinkerton, N.; Fradley, M.; Moritz, M.; Spitzer, A.; Meinke, G.; Tsai, F. T.; Sigler, P. B.; Lifton, R. P. *Science* **2000**, *289*, 119.
15. Fagart, J.; Huyet, J.; Pinon, G. M.; Rochel, M.; Mayer, C.; Rafestin-Oblin, M. E. *Nat. Struct. Mol. Biol.* **2005**, *12*, 554.
16. Pereira de Jesus-Tran, K.; Cote, P. L.; Cantin, L.; Blanchet, J.; Labrie, F.; Breton, R. *Protein Sci.* **2006**, *15*, 987.
17. Bledsoe, R. K.; Madauss, K. P.; Holt, J. A.; Apolito, C. J.; Lambert, M. H.; Pearce, K. H.; Stanley, T. B.; Stewart, E. L.; Trump, R. P.; Willson, T. M.; Williams, S. P. *J. Biol. Chem.* **2005**, *280*, 31283.
18. Williams, S. P.; Sigler, P. B. *Nature* **1998**, *393*, 392.
19. Bledsoe, R. K.; Montana, V. G.; Stanley, T. B.; Delves, C. J.; Apolito, C. J.; McKee, D. D.; Consler, T. G.; Parks, D. J.; Stewart, E. L.; Willson, T. M.; Lambert, M. H.; Moore, J. T.; Pearce, K. H.; Xu, H. E. *Cell* **2002**, *110*, 93.
20. Weichenberger, C. X.; Sippl, M. J. *Structure* **2006**, *14*, 967.
21. Dansey, M. V.; Di Chenna, P. H.; Veleiro, A. S.; Kristofikova, Z.; Chodounska, H.; Kasal, A.; Burton, G. *Eur. J. Med. Chem.* **2010**, *45*, 3063.
22. Beato, M.; Herrlich, P.; Schütz, G. *Cell* **1995**, *83*, 851.
23. Boise, L. H.; Gonzalez-Garcia, M.; Postema, C. E.; Ding, L.; Lindsten, T.; Turka, L. A.; Mao, X.; Nunez, G.; Thompson, C. B. *Cell* **1993**, *74*, 597.
24. Olopade, O. I.; Adeyanju, M. O.; Safa, A. R.; Hagos, F.; Mick, R.; Thompson, C. B.; Recant, W. M. *Cancer J. Sci. Am.* **1997**, *3*, 230.
25. Pecci, A.; Scholz, A.; Pelster, D.; Beato, M. *J. Biol. Chem.* **1997**, *272*, 11791.
26. Hillisch, A.; von Langen, J.; Menzenbach, B.; Droescher, P.; Kaufmann, G.; Schneider, B.; Elger, W. *Steroids* **2003**, *68*, 869.
27. Weichenberger, C. X.; Sippl, M. J. *Nucleic Acids Res.* **2007**, *35*, 403.
28. Simoncini, T.; Genazzani, A. R. *Eur. J. Endocrinol.* **2003**, *148*, 281.
29. Losel, R. M.; Falkenstein, E.; Feuring, M.; Schultz, A.; Tillmann, H. C.; Rossol-Haseroth, K.; Wehling, M. *Physiol. Rev.* **2003**, *83*, 965.
30. Losel, R.; Wehling, M. *Nat. Rev. Mol. Cell Biol.* **2003**, *4*, 46.
31. Riley, K. E.; Hobza, P. *J. Phys. Chem. B* **2008**, *112*, 3157.
32. Horwitz, K. B.; Zava, D. T.; Thilagar, A. K.; Jensen, E. M.; McGuire, W. L. *Cancer Res.* **1978**, *38*, 2434.
33. Kastner, P.; Bocquel, M. T.; Turcotte, B.; Garnier, J. M.; Horwitz, K. B.; Chambon, P.; Gronemeyer, H. *J. Biol. Chem.* **1990**, *265*, 12163.
34. Veleiro, A. S.; Pecci, A.; Monteserin, M. C.; Baggio, R.; Garland, M. T.; Lantos, C. P.; Burton, G. *J. Med. Chem.* **2005**, *48*, 5675.
35. Frisch, M. J.; Trucks, G. W.; Schlegel, H. B.; Scuseria, G. E.; Robb, M. A.; Cheeseman, J. R.; Montgomery, J. A.; Vreven, T.; Kudin, K. N.; Burant, J. C.; Millam, J. M.; Iyengar, S. S.; Tomasi, J.; Barone, V.; Mennucci, B.; Cossi, M.; Scalmani, G.; Rega, N.; Petersson, G. A.; Nakatsuji, H.; Hada, M.; Ehara, M.; Toyota, K.; Fukuda, R.; Hasegawa, J.; Ishida, M.; Nakajima, T.; Honda, Y.; Kitao, O.; Nakai, H.; Klene, M.; Li, X.; Knox, J. E.; Hratchian, H. P.; Cross, J. B.; Bakken, V.; Adamo, C.; Jaramillo, J.; Gomperts, R.; Stratmann, R. E.; Yazyev, O.; Austin, A. J.; Cammi, R.; Pomelli, C.; Ochtersk, J. W.; Ayala, P. Y.; Morokuma, K.; Voth, G. A.; Salvador, P.; Dannenberg, J. J.; Zakrzewski, V. G.; Dapprich, S.; Daniels, A. D.; Strain, M. C.; Farkas, O.; Malick, D. K.; Rabuck, A. D.; Raghavachari, K.; Foresman, J. B.; Ortiz, J. V.; Cui, Q.; Baboul, A. G.; Clifford, S.; Cioslowski, J.; Stefanov, B. B.; Liu, G.; Liashenko, A.; Piskorz, P.; Komaromi, I.; Martin, R. L.; Fox, D. J.; Keith, T.; Al-Laham, M. A.; Peng, C. Y.; Nanayakkara, A.; Challacombe, M.; Gill, P. M. W.; Johnson, B.; Chen, W.; Wong, M. W.; Gonzalez, C.; Pople, J. A. *GAUSSIAN 03, Revision C.02*; Gaussian, Inc.: Wallingford, CT, 2004.
36. Pearlman, D. A.; Case, D. A.; Caldwell, J. W.; Ross, W. S.; Cheatham Iii, T. E.; DeBolt, S.; Ferguson, D.; Seibel, G.; Kollman, P. *Comput. Phys. Commun.* **1995**, *91*, 1.
37. Berendsen, H. J. C.; Postma, J. P. M.; Van Gunsteren, W. F.; DiNola, A.; Haak, J. R. *J. Chem. Phys.* **1984**, *81*, 3684.
38. Cheatham, T. E., 3rd; Cieplak, P.; Kollman, P. A. *J. Biomol. Struct. Dyn.* **1999**, *16*, 845.